Tellus (1987), *39B*, 398–411

Dynamical influences on stratospheric aerosols observed at Aberystwyth in early 1983

By G. VAUGHAN, D. B. JENKINS, L. THOMAS, D. P. WAREING and M. FARRINGTON,
Department of Physics, University College of Wales, Aberystwyth, Dyfed, UK

(Manuscript received 9 June; in final form 3 November 1986)

ABSTRACT

An intensive study of stratospheric aerosols by means of a lidar (laser radar) was conducted at Aberystwyth (52.4°N, 4.1°W) during February and April 1983, when the optical depth due to aerosols associated with the El Chichon eruption was greatest. Very sharp vertical gradients in the aerosol backscatter profile (factors of 7 in 100 m) were found to accompany the onset and decay of a block in the tropospheric flow, and to be related to the proximity of the polar stratospheric vortex. Differential advection, identified as the process most likely to be responsible for such gradients, is suggested as a mechanism for the erosion of stratospheric vortices isolated from the pole by vigorous planetary wave activity. Statistical studies of the aerosol data reveal a time scale of 36–48 hours for temporal coherence above 17 km, corresponding to a length scale of about 300 km for the dominant irregularities in the cloud. Irregularities below 17 km were much smaller both in amplitude and scale. The observations of very sharp gradients in the aerosol cloud, facilitated by the excellent vertical resolution of the lidar technique (30 m), reveals interesting wave-like perturbations possibly caused by a gravity wave.

1. Introduction

From November 1982 until December 1984, the lidar system at the University College of Wales, Aberystwyth (52.4°N, 4.1°W) was used to observe the stratospheric aerosol layer resulting from the eruption of El Chichon in March and April 1982. The lidar was based on a neodymium-YAG laser, frequency-doubled to 532 nm and therefore sensitive to the larger particles in the aerosol size spectrum (Hofmann and Rosen, 1984). Preliminary results from this system were presented by Thomas et al. (1983), and a full description together with results from the first two years' measurements is given by Thomas et al. (1987). Aerosol measurements presented in this paper are mostly in the form of aerosol backscatter ratio, defined as

$$R - 1 = \beta_a(h)/\beta_m(h) \qquad (1)$$

where $\beta_a(h)$ and $\beta_m(h)$ are the differential volume backscatter coefficients at height h due to aerosols and molecules, respectively. It resembles somewhat an aerosol mixing ratio, but there are important differences, discussed in detail in Section 3. During the period up to April 1983, incomplete overlap of the transmitted beam with the receiver's field of view precluded accurate aerosol measurements below about 12 km, thus the results reported here are restricted to heights above 12.15 km.

It seems that November 1982 marked the arrival of the main aerosol cloud at Aberystwyth (Thomas et al., 1987) and although extensive measurements were made with the lidar during that month the results showed such large and rapid variability (often within a night) that no coherent pattern could be discerned. This study of short-term variations in the aerosol layer therefore concentrates on the months of February to April 1983, when the variability had decreased and consistent features could be identified over several measurements. Particularly favourable observing conditions were enjoyed during these two months, with measurements obtained on 13 nights in February and 12 nights between March 25 and April 30. Several observations were conducted on many of these nights, with independent measurements separated by as little as 20 minutes.

The period February–April 1983 corresponded to maximum values of aerosol optical depth seen at Aberystwyth due to the El Chichon eruption (Thomas et al. 1987). The resulting combination of good measurement precision and frequent observation makes these data ideal for a study of the role of atmospheric dynamics in the variability of the aerosol layer. This is illustrated by contrasting two periods (February and April) with different wind regimes and by examining statistical correlations of the backscatter observations to determine coherence lengths and characteristic variability. Particular consideration is given to the influence of the polar vortex on the aerosol measurements, especially with respect to very sharp vertical gradients in backscatter ratio.

2. Meteorological background

Meteorological conditions in the lower stratosphere during February 1983 were markedly different from those of late March and April. This is illustrated in the synoptic description of the winter of 1982/83 in the Northern Hemisphere stratosphere presented by Naujokat et al. (1983). February is shown as a very disturbed month, with planetary wave activity reaching a maximum during the first three days and again from the 15th to the 20th. A reversal in the 30 mb zonal mean temperature difference between 60°N and the pole occurred on February 7 and again from February 26 to March 1, although a reversal of the circulation (a major warming) did not take place. In the vicinity of the UK this activity was manifest as the stratospheric extension of intense blocking in the tropospheric flow, with a strong meridional component to the winds. Indeed, high pressure at the surface associated with the block was responsible for the excellent observing conditions during February. Lejenäs and Økland (1983) identified blocking with a negative value of the zonal index—the geopotential height difference between 40°N and 60°N at a given longitude—on the 500 mb surface. Values of this index taken from meteorological charts (Deutscher Wetterdienst, Offenbach) at 0° longitude are shown in Fig. 1, together with the corresponding index for the 50 mb surface and the 50 mb wind vector reported by the radiosonde at Camborne (50.5°N, 5.0°W). The 50 mb (~20 km) surface was near to the peak of the aerosol backscatter ratio throughout most of February (see below). Strong correlation between the zonal indices plotted in Fig. 1 demonstrates that changes in the circulation at 50 mb were closely linked to disturbances in the troposphere. By Lejenäs and Økland's criterion, blocking was present from February 8–19, with the zonal component of the 500 mb flow remaining weak until the end of the month. Thus, the first two nights of aerosol observations, February 2/3 and 3/4, differed from those which followed: the very strong westerly winds at 50 mb contrast markedly with lighter, more meridional and variable winds seen during the rest of February.

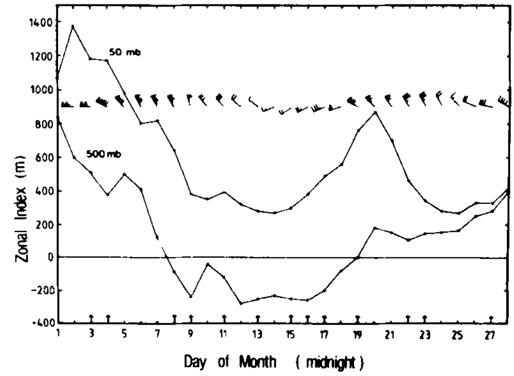

Fig. 1. Zonal index (Z(40°N) − Z(60°N) where Z represents geopotential height) at 0° longitude on the 500 and 50 mb surfaces for February 1983. Wind flecks denote the 50 mb wind vectors in knots, measured by the Camborne radiosonde at midnight (adjacent stations were used when Camborne data were not available). Arrows along the date axis mark the nights on which aerosol observations were made.

Vigorous planetary wave activity is a powerful agent for meridional mixing of air, as recent observations of potential vorticity distributions have shown (McIntyre and Palmer, 1983; Clough et al., 1985). The disturbed conditions during February could therefore have been expected to bring air from a variety of different latitudes to

Aberystwyth. In fact, this was not the case: an examination of synoptic charts showed that most of the air sampled by the lidar between 12 and 20 km had travelled from a more northerly latitude in the previous two days. Without the facilities for accurate trajectory calculations specific air parcel origins could not be determined; however, not one occasion could be identified during February when air of recent (1–2 days) subtropical origin could have reached Aberystwyth at any altitude between 14 and 23 km (200 and 30 mb). It must then be concluded that our measurements represent, for the most part, air on the outer fringe of the polar stratospheric vortex.

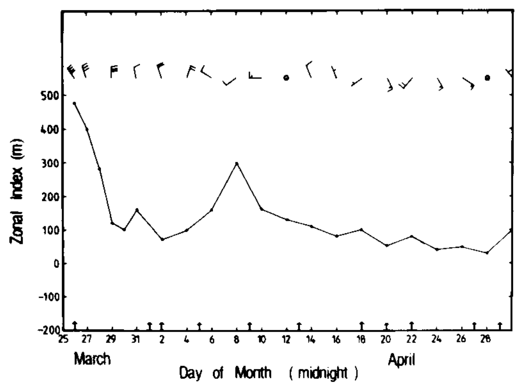

Fig. 2. Zonal index at 0° longitude on the 50 mb surface for the period March 26–April 30 1983. Wind flecks and arrows along time axis are as for Fig. 1. (Note different scale to Fig. 1.)

The spring reversal in the lower stratosphere was very gradual in 1983 (Naujokat et al., 1983), with a very weak zonal component to the flow throughout April. Near the UK, the zonal index at 50 mb decreased rapidly at the end of March and remained between 0 m and 200 m throughout April except for the 8th, as shown in Fig. 2. Winds over Camborne were very light and variable, showing that meridional flow was also very weak during this period. Under these conditions there would be no benefit in attempting to calculate air parcel trajectories as the lack of a synoptic scale pressure gradient allows smaller scale features to dominate the flow.

3. Broad features of the aerosol cloud

Profiles of aerosol backscatter ratio observed during February could be divided into five broad categories, illustrated in Fig. 3. The month began with very small aerosol amounts, located mainly below 16 km. Pronounced layering of the profiles was seen on the 7/8 and 18/19 February, corresponding to the onset and decay of the tropospheric block. During the periods when zonal

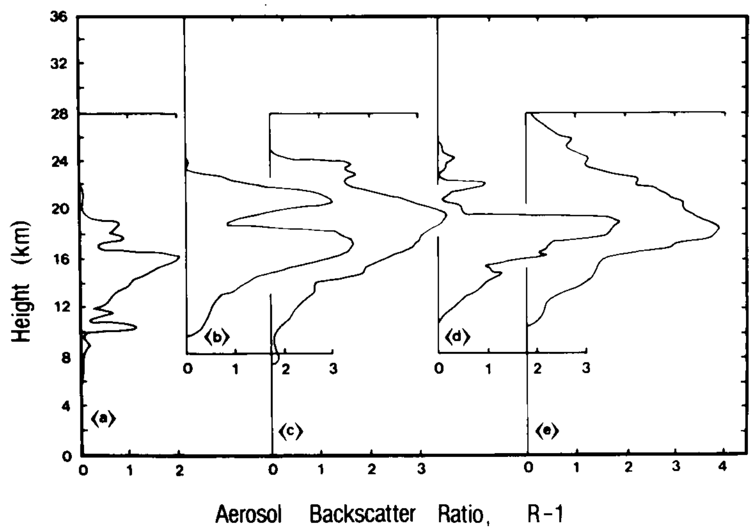

Fig. 3. Categories of aerosol backscatter ratio (R-1) profiles observed during February 1983, with vertical resolution 300 m: (a) night of 3/4 February; (b) night of 7/8 February; (c) night of 8/9 February; (d) night of 18/19 February; (e) night of 22/23 February.

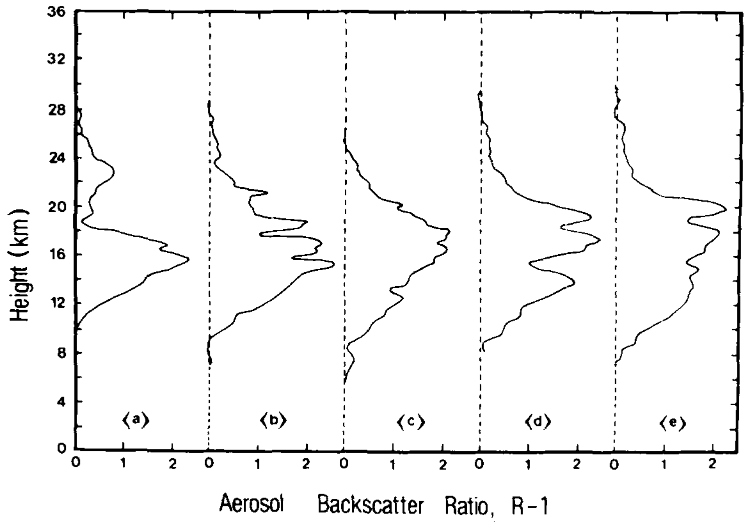

Fig. 4. Categories of aerosol backscatter ratio (R-1) profiles observed during March/April 1983, with vertical resolution 300 m: (a) night of 25/26 March; (b) night of 31 March/1 April; (c) night of 8/9 April; (d) night of 17/18 April; (e) night of 26/27 April.

flow at 50 mb was relatively weak and unchanging, vertical gradients of aerosol concentration were much less pronounced, and large values of the aerosol backscatter ratio were observed, peaking between 19 and 20 km.

The profiles in Figs. 3c and 3e are representative of most of the observing nights during February and show a fairly smooth vertical profile. In fact, the February profiles, generally, show less small-scale vertical structure than those of late March and April (Fig. 4). Peak values of the aerosol backscatter ratio during April rarely exceeded 2.5, but an increase in the ratio below 15 km implied that the average aerosol optical depth above 12.15 km (0.121 ± 0.003) was not substantially smaller than that of February (0.15 ± 0.1). As with the February data, the first profile of the second period (March 25/26) shows an anomalously low aerosol content above 17 km, except for a secondary peak at 23 km. Both periods therefore displayed a fairly homogeneous aerosol layer when there was little potential for long-range transport (i.e., winds were light), interspersed with profiles of a very different character when the zonal index at 50 mb exceeded 500 m.

It must be recognized that there is no obvious relationship between the aerosol backscatter ratio and the aerosol mass mixing ratio, since the lidar technique is sensitive only to the larger aerosol particles ($r > 0.1$ μm). In-situ measurements from Laramie (41 °N) showed that the mean radius of volcanic aerosol particles between 17 and 25 km was in the range 0.15–0.25 μm in the spring of 1983 (Hofmann and Rosen, 1984), with an increased fraction of smaller particles ($r < 0.15$ μm) below 15 km (Hofmann et al., 1985). It is not then unreasonable to suppose that most of the mass of the aerosol layer was concentrated in particles with $r > 0.15$ μ. Such particles would be visible to the lidar at 532 nm. The exact relationship between backscatter ratio and mass mixing ratio is a function of the droplet size spectrum, and since both this and the mixing ratio itself vary with temperature and ambient humidity, changes in the backscatter ratio with time could be interpreted either as advection of aerosol or changes due to evaporation and condensation. An extreme example of the latter process is presented by Hofmann et al. (1985), where evaporation of aerosol droplets by a stratospheric warming at 30 km was followed by condensation as very small particles which would have been invisible at 532 nm. At the heights considered here, however, evaporation of the aerosols did not occur. We can therefore apply the result of Pinnick et al. (1980), who showed that, for sulphuric acid aerosols smaller in radius than twice the laser wavelength, an approximately linear relationship holds between backscatter and aerosol mass content. (These calculations were performed at 694 nm and 1.06 μm but the conclusions should be broadly applicable at 532 nm.)

The range of temperatures at 50 mb corresponding to the February observations fell into two categories: −75°C to −73°C on 2/3, 3/4 and 18/19 and −67°C to −55°C on the other nights. As expected from the reduced dynamical activity, less variation was seen in the second period: −57°C on March 26 and −54°C to −48°C during April. Calculations of aerosol growth presented by Steele et al. (1983) show the droplet radius to be a very insensitive function of temperature above −67°C for representative stratospheric humidities: a change of temperature from −67°C to −55°C, for instance, causes a change of less than 5% in the aerosol radius, and thus less than 15% in the mass content and backscatter (Pinnick et al., 1980). Greater sensitivity to temperature is expected below −73°C, but the observed variation of 2°C on 2–4 February would have led to a change of less than 3% in the droplet radius according to the calculation of Steele et al. Individual aerosol profiles were compared with radiosonde temperature profiles measures on the same night at Camborne, but no correlation was found, except for a suggestion in the February data that the top of the aerosol layer coincided with an increase in the vertical temperature gradient. Variations in the backscatter ratio are therefore best attributed to the advection of an inhomogeneous aerosol cloud, and specific features of the observations will be discussed in the light of this interpretation.

3.1 *Proximity of the polar night vortex*

Results from both satellite observations and airborne lidar studies have shown depleted aerosol concentrations in the stratospheric polar vortex. In studies of pre-El Chichon aerosols, Kent et al. (1985) reported a depletion in the background stratospheric aerosol above 14 km in the early winter, when the vortex is still symmetric about the pole, while Wang and McCormick (1985) showed that the depletion persisted above 50 mb in isolated cyclonic vortices displaced from the pole later in the winter by planetary waves. Large potential vorticity gradients, found near the maximum in the polar night jet, inhibit horizontal mixing of aerosol into the polar vortex, and subsidence of air in the vortex due to radiative cooling was identified as a removal mechanism for the aerosol by Kent et al. (1985). Nights when Aberystwyth lay within or near the edge of the polar vortex should therefore have shown unusually low backscatter ratios.

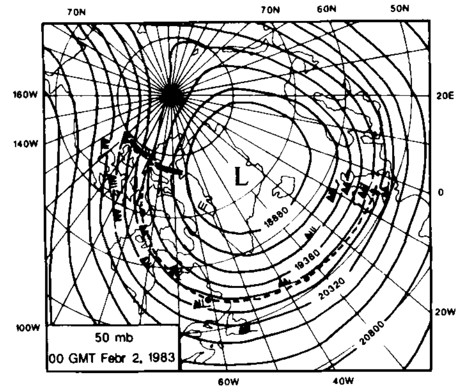

Fig. 5. 50 mb geopotential height chart for 00 GMT, February 2, 1983. Contour values are given in m with contour separation 160 m. The flight path reported by McCormick et al., (1983) is shown as a double line extending westward from Thule (76.5°N, 68.7°W). Aberystwyth (52.4°N, 4.1°W) is denoted by a cross. The dashed line shows the back trajectory calculated on the 50 mb surface from 00 GMT February 3, 1983 at Aberystwyth; dots on this line represent 12 hour intervals. Radiosonde winds are plotted in knots according to the usual meteorological convention.

McCormick et al. (1983) showed that El Chichon aerosol penetrated the polar vortex in the autumn of 1982 below 18 km but was absent above this height. Following Kent et al. (1985), charts for 30 mb and 50 mb on the observing nights were examined to determine the position of the polar night jet. Five occasions were identified when the jet maximum lay either to the south or within 200 km to the north of the observing site: 2/3, 3/4, 7/8 and 18/19 February and 25/26 March. It is clear from Figs. 3 and 4 that, other than 7/8 February, these dates do indeed correspond to low aerosol amounts above 18 km, but that the depletion is not confined to these heights.

The observations on 2/3 February and 3/4 February may be compared directly with those reported by McCormick et al. (1983) from a flight due west from Thule, Greenland (76.5°N, 68.7°W) on 1 February with an airborne lidar using a wavelength of 694 nm. The 50 mb chart for 00 GMT February 2, 1983 is shown in Fig. 5,

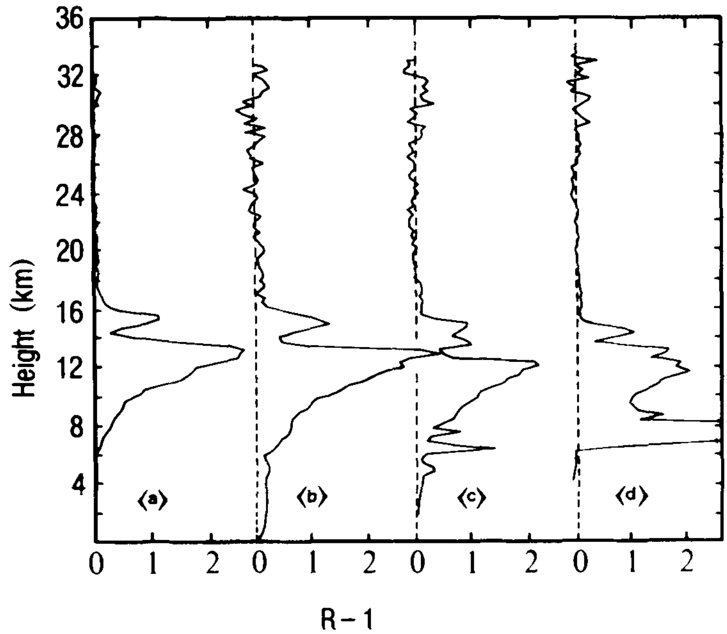

Fig. 6. Profiles of the aerosol backscatter ratio observed during the early part of February, with vertical resolution 300 m: (a) 23.15 GMT on February 2, 1983; (b) 03.25 GMT on February 3, 1983; (c) 19.40 GMT on February 3, 1983; (d) 07.26 GMT on February 4, 1983. Enhanced backscatter on the last two profiles below 10 km was caused by cirrus clouds.

with the flight path reported by McCormick et al. Also shown is a back-trajectory estimate, beginning from Aberystwyth at 00 GMT on February 3, 1983 and calculated according to the method of Reiter (1972), with the added assumption that there was no vertical wind shear along the trajectory. This assumption allowed winds on the 50 mb chart (rather than the corresponding isentropic surface) to be used to define the trajectory; vertical displacements could then be estimated from

$$\Delta z = -g/C_p \, \Delta T$$

where ΔT was the change in temperature along the isobaric trajectory. This method assumes further that the lower stratosphere was nearly isothermal, a reasonable assumption on the day in question, as indeed was the assumption of no vertical wind shear.

Even from such a rough trajectory estimate, it is clear that air sampled along the flight track on 1 February would reach the UK on the night of 2/3 February. (A more sophisticated trajectory calculation would not be of much assistance in this case, given that only two radiosonde observations were available between North America and the UK.) The vertical displacement is estimated as +1.8 km between the Canadian Arctic and Aberystwyth.

The lidar profiles of McCormick et al. within the vortex show an aerosol layer confined below 18 km, with peak backscatter ratio (at 694 nm) greater than 4 at 16 km, while outside the vortex several layers were seen, the main one showing a backscatter ratio of 2 at 15 km, with substantial aerosol amounts above 20 km. Intermediate profiles showed a gradual change from one type to the other as the polar night jet was crossed. Consistent with the trajectory estimate, backscatter ratio profiles observed at Aberystwyth in the period 2–4 February (Fig. 6) are in very satisfactory agreement below 20 km with the airborne measurements near the middle of the flight track, when the allowance is made for the vertical displacement along the trajectory and the difference in laser wavelength. However, these observations near the middle of their flight track also showed a considerable amount of aerosol above

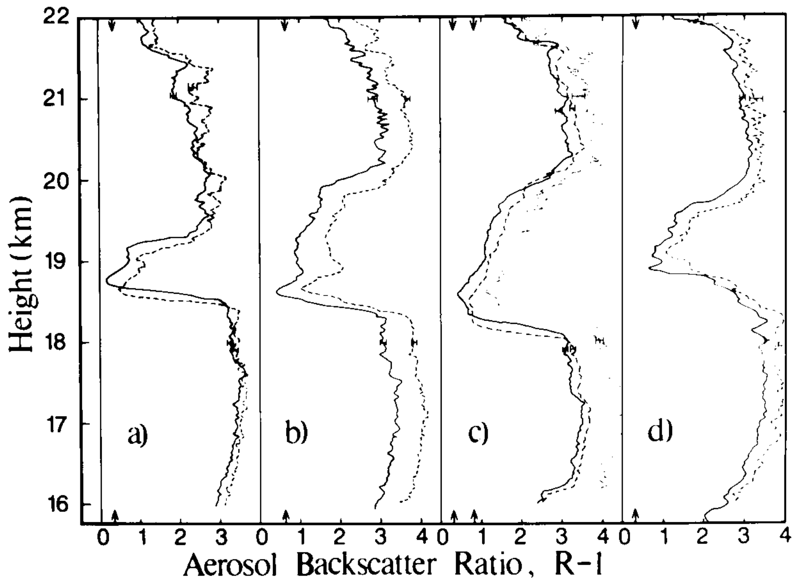

Fig. 7. Profiles of aerosol backscatter ratio with 30 m height resolution obtained on the night of 7/8 February 1983. The data were obtained in four groups, each profile covering a 20-min period ending at: (a) 18.42 GMT and 19.03 GMT on February 7, 1983; (b) 23.34 GMT on February 7, 1983 and 00.13 GMT on February 8, 1983; (c) 03.11 GMT, 03.31 GMT and 03.58 GMT on February 8, 1983; (d) 07.10 GMT and 07.31 GMT on February 8, 1983. The full line in each group represents the first profile and is drawn to the scale on the abscissa. Subsequent profiles, represented in turn by dashed and dotted lines, have been displaced by an amount represented by the arrows on the abscissae. Error bars representing one standard deviation either side of each profile have been drawn near 18 and 21 km.

20 km, indicative of measurements outside the stratospheric polar vortex (Wang and McCormick, 1985). This feature was entirely absent from the Aberystwyth data during 2–4 February, whilst those airborne measurements within the vortex and free of aerosol above 20 km do not resemble the Aberystwyth profiles at the lower heights; they do not, for instance, show a double peak. Differential advection between the 30 mb and 50 mb surfaces can clearly account for this (the available meteorological data were too sparsely distributed for a trajectory estimate at 30 mb), but the two sets of profiles do suggest that the polar vortex (certainly below 20 km) is not advected as a rigid cylinder. The close vertical proximity of air originally outside the vortex with air apparently within it is indicative of a sloping boundary to the vortex, and therefore to the polar night jet. This increases the potential for exchange of air across the jet by small-scale mixing and therefore to the erosion of the polar vortex—a process presumably facilitated by a very disturbed stratospheric circulation as in the present case.

3.2 Pronounced layering of the aerosol profiles

Also measured near the polar night jet were the remarkable profiles of 7/8 February and 18/19 February, Fig. 3. On the 7/8th, as shown in Fig. 7, the backscatter ratio fell from 3.5 to less than 0.5 in 100 m, while a similar fall occurred on the 18/19th in 150 m. Under the influence of vertical turbulent diffusion an initial step function in the aerosol backscatter ratio at height z_0 will evolve according to

$$(R(z, t) - 1) \propto 1 - \operatorname{erf} \frac{(z - z_0)}{2(Kt)^{1/2}}$$

(Jeffreys and Jeffreys, 1972, p. 566), where K is the diffusion coefficient. A decrease in aerosol concentration to near-zero values in about 100 m then corresponds to $Kt \sim 1000\ \mathrm{m}^2$. Estimates of K_h, the vertical heat diffusion coefficient in small-scale patches of turbulence in the lower

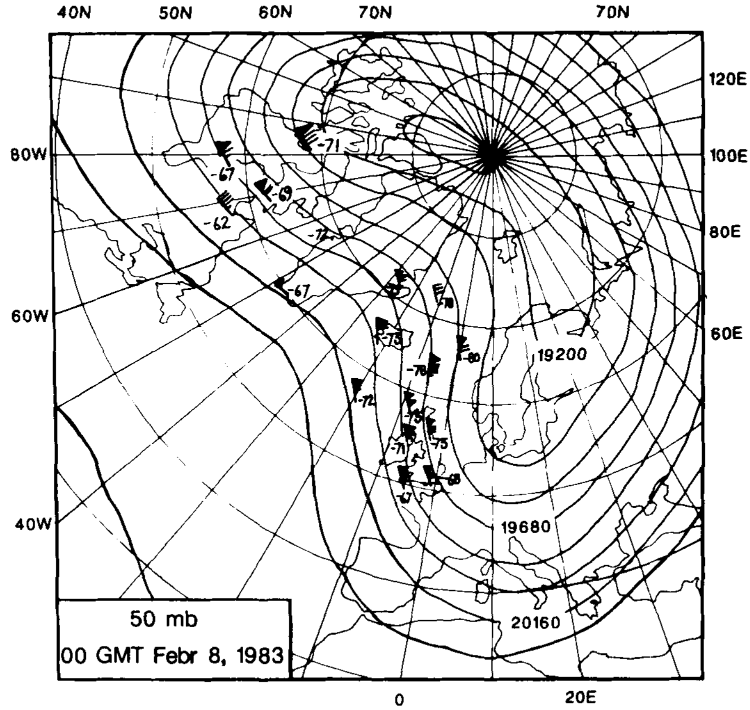

Fig. 8. 50 mb geopotential height chart for 00 GMT February 2, 1983. Contour values are given in m, with contour separation 160 m. Wind vectors have been plotted upstream of Aberystwyth in the same manner as for Fig. 5, with temperatures in degrees C.

stratosphere, range from 10^{-2} ms^2 s^{-1} (Cadet, 1977) to 1.0 m^2 s^{-1} (Heck, 1977). Taking this range as applicable to aerosol redistribution we find an upper bound on the lifetime of the strong gradient seen on February 7/8 of about 1 day. The likely origin of the air containing the aerosol-free layer may be discerned from the 50 mb chart for midnight on 8 February, shown in Fig. 8. The ridge over Greenland and Iceland (forced by the block in the tropospheric flow) was intensifying at this time, causing an elongation of the polar vortex and a deep trough over Scandinavia. Since the amplitude of the trough-ridge pattern was also decreasing with increasing height, conditions were ideal for modifying the aerosol profiles by differential advection. However, for this process to generate such a sharp vertical gradient, the undisturbed aerosol concentrations must have contained a sharp horizontal gradient near the polar night jet stream—somewhat at variance with the gradient reported by McCormick et al. (1983). It is worth considering the alternative hypothesis that the aerosol-free layer was caused by the condensation of polar stratospheric clouds (McCormick et al., 1982), followed by gravitational settling.

Very strong northerly winds imply that the air over Aberystwyth had travelled from the Greenland/Iceland area in the previous 24 hours, with considerable subsidence revealed by the marked horizontal temperature gradient. Air over Aberystwyth at midnight on the 8th February would have passed near to Scoresbysund on the East Greenland coast (70.5°N, 22°W) about 12 hours previously. The temperature profile measured there at 12.00 GMT on the 7th showed very cold temperatures in the lower stratosphere. Assuming adiabatic flow, air on the 50 mb surface 12 hours later would have descended from about 40 mb over Scoresbysund. This puts the altitude of the aerosol-free layer at about 19.6–21.0 km 12 hours prior to the measurements, with temperatures ~ -81 °C. Satellite observations reported by McCormick et al. (1982) showed that polar stratospheric clouds can be formed near 50 mb when the temperature is colder than −75°C. Condensation can indeed occur within a fairly narrow layer, and could be responsible for precipitation of the aerosol particles out of the layer.

On close inspection, however, this process appears unlikely. Even if temperatures of −81°C were encountered by the air, it is clear from Fig. 8 that this could only have occurred between Scoresbysund and Stornoway (58.2°N, 6.4°W) in the previous 24 hours. With the reported wind speeds this region would have been traversed in about 10 hours by an individual air parcel. Calculations of the growth of aerosol particles in polar stratospheric clouds have been presented by Steele et al. (1983). They showed that aerosol at 100 mb with initial radii 0.29 μm grow very rapidly to radii near 4 μm as the temperature falls below −80°C, with 6 p.p.m.v. ambient humidity. Their calculations of the extinction of solar radiation with 1 μm wavelength under solar occultation conditions agreed with corresponding measurements by the SAM-II satellite, allowing them to deduce a typical mixing ratio of 6 p.p.m.v. for water vapour in the Arctic winter stratosphere. This agreement suggests that their model for particle growth is not substantially in error. Condensation at −80°C converts almost all the ambient water vapour to the liquid or solid phase, prohibiting further growth by condensation at still lower temperatures. Particle growth can proceed by coalescence in a cloud, but this process is slow for such small particles, and was not considered by Steele et al. (1983). The mean radius of the El Chichon aerosol was less than 0.29 μm and the absolute humidity at 50 mb half that at 100 mb for the same water vapour mixing ratio. Thus, the mean radius of cloud particles condensing at 50 mb in the present case would be somewhat less than 4 μm (Steele et al., 1983). Particles with radii 3 μm would take 73 hours to fall 500 m at 50 mb (Kasten, 1968), far longer than the time an individual air parcel would have spent within the cloud. It is therefore most unlikely, given the upper bound of a day previously estimated for the lifetime of the very sharp backscatter gradient, that the aerosol-free layer was formed by the gravitational settling of a stratospheric cloud.

Radiosonde wind measurements upstream from Aberystwyth were examined for the period 00 GMT on the 7th February to 00 GMT on the 8th for evidence of a shallow layer near 50 mb with marked wind shear at its edges. Unfortunately the radiosonde network is sparse in the north-east Atlantic, and wind measurements in the lower stratosphere are difficult to obtain in strong winds when the balloon is near the horizon. Most of the wind measurements, in fact, either ceased below 70 mb or were reported only at standard levels thereafter. Of the remainder, there was slight evidence of wind shear at Scoresbysund at 12.00 GMT (directions of 310° at 50 and 30 mb and 315° at 38.5 mb), stronger evidence at Lerwick (60.1°N, 1.2°W) at 12.00 GMT (directions of 355° at 50 mb, 345° at 38.8 mb, 355 at 32.8 mb and 340 at 30 mb), and no evidence at Stornoway or Keflavik (64.0°N, 22.6°W) at 12.00 GMT. These wind profiles, sparsely distributed in space and time, neither confirm nor deny that the aerosol-free layer was a product of differential advection, but this hypothesis remains much more likely than that involving condensation.

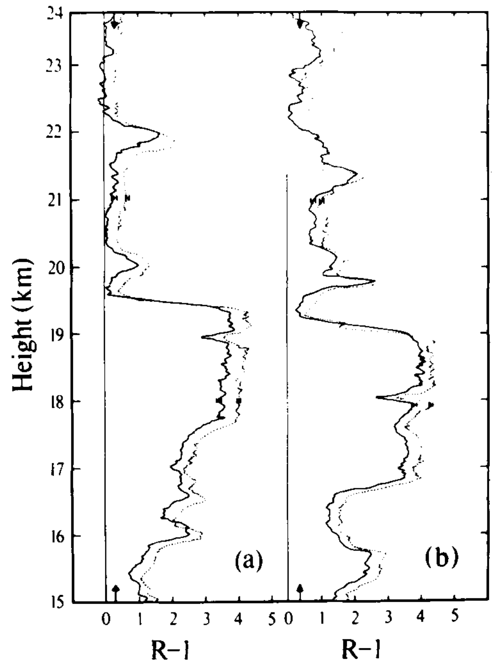

Fig. 9. As Fig. 7, except for the night of 18/19 February 1983. (a) 21.12 GMT and 21.30 GMT February 18, 1983. (b) 06.18 GMT and 06.39 GMT February 19, 1983.

A similar sharp gradient in aerosol backscatter was observed on the night of 18th/19th February, again near 50 mb (Fig. 9). This time, temperatures upstream from Aberystwyth exceeded −72°C for at least the previous 24 hours, so condensation could have played no part in its formation. This gradient again occurred during a period favouring large-scale differential advection, as the block in the tropospheric flow weakened (Fig. 1). The inevitable erosion of such gradients by small-scale mixing provides a mechanism for redistribution of tracers, and presumably also of potential vorticity if its correlation with aerosol persists near the polar night jet, as observed by Kent et al. (1985) and McCormick et al. (1983).

The aerosol data therefore suggest that during vigorous planetary wave activity, differential advection of tracers can promote mixing by setting up very sharp vertical gradients. This mechanism may be a significant factor in the dissipation of potential vorticity anomalies drawn from polar regions by amplifying planetary waves, as reported by McIntyre and Palmer (1983) and Clough et al. (1985).

4. Statistical studies of the aerosol layer

To study the variability of the aerosol layer and its temporal and altitudinal coherence, the backscatter profiles were divided into eight height intervals from 12.15 to 22.65 km and aerosol optical depths calculated for each interval. Separate statistical studies were then conducted for February and April. To ensure a reasonably homogeneous set of data, measurements strongly affected by the position of the polar vortex (2–4 February and 25/26 March) were excluded: profiles for February 7/8 and 18/19 were not excluded since aerosol amounts were large on both nights despite the remarkable vertical structure. Thus the statistical studies for both months apply to aerosol layers on the equatorward side of the polar night jet under conditions of weak zonal flow in the lower stratosphere.

4.1. *Variability*

The distribution of profiles with time was very uneven (Figs. 1, 2) and changes within a night were generally considerably less than those seen from night to night (Subsection 4.3). Large numbers of profiles taken on the same night could, therefore, bias estimates of the variability, and to eliminate this possibility all data obtained in a given height interval on the same night were averaged. Mean values and standard deviations of the optical depth in each height interval were then calculated for the two periods: 8–28 February 1983 and 1–30 April 1983, as shown in Table 1. Use of a month's data after taking an average for each night restricts the time scales contributing to the variability largely to those associated with synoptic scale disturbances in the troposphere (2–10 days).

One prominent feature of Table 1 is the fall of the aerosol layer between February and April. Although the total aerosol optical depth between 12.15 and 22.65 km decreased from 0.151 to 0.121 this disguises a sharp decrease from 0.102 to 0.057 above 15.75 km and an increase from 0.029 to 0.044 below 14.55 km, a fall in the centre of mass of 2.1 km. With a mean radius of $\sim 0.2\ \mu m$ for the aerosol, as argued earlier, the calculations of Kasten (1968) suggest a fall of ~300–400 m in 2 months. Gravitational settling alone cannot, therefore, explain the observed decrease in altitude.

Despite the differences in the overall aerosol profiles, the fractional standard deviations were remarkably consistent between February and April. Variability increased with height up to 15.75 km, then fell to a minimum before increasing again above 18.15 km (except for the highest interval in April). Although the height of minimum variability, 15.75–18.15 km, corresponded to the peak optical depth in February this was not so in April, nor was the peak backscatter ratio situated in this region in February. Variability was therefore not correlated with vertical gradient in optical depth or backscatter ratio and cannot be explained simply by fluctuations in the height of the aerosol layer.

4.2. *Coherence with altitude*

The coherence of the aerosol cloud with altitude was examined by calculating the correlation coefficients between optical depth values in different height intervals. The February data showed a distinct pattern, with all layers above 16.95 km correlating significantly with one another at the 95% level or greater and no layer below 16.95 km doing so with any other. In contrast, the only two significant correlations in April were between layers 1 and 2 ($r = 0.81$) and

Table 1. *Means and standard deviations of the aerosol optical depth measurements*

Height interval index	Height interval (km)	No. profiles included	Mean optical depth ($\times 10^3$)	Standard deviation ($\times 10^3$)	Fractional standard deviation
(1) February 1983					
1	12.15–13.35	9	11.9	1.5	0.13
2	13.35–14.55	9	16.7	3.2	0.19
3	14.55–15.75	10	20.3	4.3	0.21
4	15.75–16.95	11	25.7	2.8	0.11
5	16.95–18.15	11	26.4	2.5	0.09
6	18.15–19.35	11	22.2	4.8	0.21
7	19.35–20.55	11	14.2	3.8	0.27
8	20.55–22.65	11	13.6	3.7	0.27
(2) April 1983					
1	12.15–13.35	10	22.2	2.8	0.13
2	13.35–14.55	10	21.9	2.6	0.12
3	14.55–15.75	10	19.6	4.0	0.21
4	15.75–16.95	10	19.1	2.3	0.12
5	16.95–18.15	10	15.5	1.8	0.12
6	18.15–19.35	10	10.8	1.8	0.17
7	19.35–20.55	10	7.1	2.4	0.34
8	20.55–22.65	10	4.3	0.5	0.13

4 and 8 ($r = 0.70$). Finer vertical structure is evident in the April profiles in Fig. 4, presumably due to the differential advection mechanism previously discussed.

4.3. *Temporal coherence*

The temporal coherence was studied by calculating the autocorrelation coefficient $\varepsilon(\tau)$ for optical depth data in each layer. This study was only performed for the February data since those for April were spread over a longer period and were even less regularly spaced.

Because of the uneven temporal distribution of the data care had to be taken once more to ensure that the autocorrelation coefficients were not excessively biased. ε for $0 < \tau \leqslant 2$ hours was always very high (>0.84 in all cases and >0.95 in most) and significant at the 99% level, as shown in Table 2. Inclusion of a group of three or more points less than two hours apart in the calculation of ε for greater lags would therefore give an undue weighting to (effectively) one profile. To calculate ε for such lags, therefore, optical depths of profiles closer than 2 hours in time were averaged.

Above 19.35 km, the results were clear-cut. For $\tau < 36$ hours, ε was significant at the 99% level and for $\tau > 48$ hours it was not significant even at the 95% level; no value of ε was available from 36 to 48 hours. This clearly identifies 36–48 hours as a kind of 'coherence time' for the top part of the aerosol cloud during this period. Below 14.55 km, the only significant value of ε was that for $\tau < 2$ hours, but because of the sparser data coverage at these altitudes an insufficient number of profiles (<5) were available for the significance test for lags < 48 hours. In the other four layers conclusions are less easy to draw, but there is some impression of an increase in coherence time with altitude.

These three statistical studies reveal a definite pattern in the structure of the aerosol cloud during February. Above about 17 km, changes in the aerosol amount were vertically coherent although they increased significantly in amplitude with increasing height. A time scale of about 36–48 hours for temporal coherence above about 19 km points to a horizontal length of ~ 3000 km for the dominant irregularities in upper part of the cloud, taking an average wind speed of about

Table 2. *Significance level of autocorrelation coefficients at different lag intervals (%)*

Lag interval (hours)	Height interval (km)							
	12.15–13.35	13.35–14.55	14.55–15.75	15.75–16.95	16.95–18.15	18.15–19.35	19.35–20.55	20.55–21.65
0–2	>99	>99	>99	>99	>99	>99	>99	>99
2–6			NS	NS	>95	>95	>99	>99
6–12			NS	>99	>99	NS	>99	>99
12–18				>99			>99	
18–24			>99	NS	>99	NS	>99	>99
24–36			NS	NS	>99	NS	>99	>99
36–48								
48–72	NS	NS	NS	NS	NS	NS	NS	NS
72–96	NS	NS	NS	>95	NS	>99	NS	NS
96–120	NS	NS	NS	NS	NS	NS	NS	NS
120–144	NS	NS	NS	NS	NS	>95	NS	NS
144–168	NS	NS	NS	NS	NS	NS	NS	>95

Significance levels are shown rather than values of ε since the number of profiles included is different in each case. No entry means that fewer than 4 pairs of profiles were available to calculate the autocorrelation. NS represents a significance level less than 95%, i.e., not statistically significant,

$20\ \mathrm{ms^{-1}}$ (Fig. 1). In contrast, the very much smaller amplitude irregularities seen below 17 km appear also to exhibit very much smaller coherence length in both vertical and horizontal directions. The change between the two regions is fairly abrupt and is shown in all three studies.

5. Very rapid changes of small features in the aerosol layer

The discussion up to this point has been concerned with vertical scales of a kilometre or more. The lidar system has a vertical resolution of 30 m, and on occasions when a number of observations were made in quick succession this enabled the persistence of very small vertical scale features in the aerosol cloud to be investigated. On most nights such features were not discernible from the experimental noise, but two examples are presented when very distinctive features were present which could readily be tracked from profile to profile. These are the sharp "ledges" present in the layered profiles on February 7/8 and 18/19.

5.1. 7–8 February 1983

The evolution of the aerosol-free layer discussed in Section 3 is clearly shown in the sequence of profiles measured during the night, Fig. 7. The ledge at the bottom of this layer persisted from 18.40 GMT on 7 February to 04.00 GMT on 8 February—corresponding to a length of at least 1200 km with the observed wind speed of $37\ \mathrm{ms^{-1}}$. Definite variations are clearly seen in the height of the ledge, particularly in the set of three profiles taken between 03.11 GMT and 03.58 GMT, Fig. 7c. These variations can be examined by matching the patterns of successive profiles in an altitude region of about 1 km and noting the height displacement: the accuracy of this procedure is comparable to the resolution of the profiles, i.e., 30 m.

The changes in altitude of features in the aerosol cloud may be interpreted simply as changes in the morphology of the cloud as it advected past the observing site, with no changes in the background atmosphere. Alternatively, one can consider the features as being tied to a particular isentropic surface and use the aerosol cloud as a tracer of dynamical influences on that surface. Without coincident high-resolution temperature profiles there is no unambiguous way of discriminating between these two possibilities, but given the almost identical shape of the three aerosol profiles between 03.11 GMT and 03.58 GMT, the evidence points strongly in favour of the second, at least on very short time scales.

The three profiles in Fig. 7c reveal what appears to be a wave pattern in the height variation. The lower edge of the aerosol-free layer, initially centred on 18.2 km, fell by 120 m, then returned to its original position. At 20 km the upper edge of the layer rose by 100 m then fell slightly, whilst the small features at 21.6 km fell initially by 70 m and then subsequently by a small amount. The small nose at 21.6 km was less distinctive than the other two features, and its identification on the 03.58 GMT profile, in particular, needs to be regarded with some caution.

One possible explanation of the wave pattern is a gravity wave with a period of about 2 hours and vertical wavelength of about 4 km. Such a wave would have a horizontal phase velocity of about 14 ms^{-1} relative to the wind and a horizontal wavelength of about 100 km. With the information from these profiles alone, we cannot demonstrate unambiguously that a gravity wave was observed; however, this analysis does illustrate the potential of high-resolution aerosol measurements in studies of small-scale dynamics.

The hypothesis that features in the cloud are tied to isentropic surfaces is supported by the slow descent of the lower edge during the course of the night. The 450 K surface was very near to the edge and this surface fell by 400 m over Camborne in the 24 hours from 12.00 GMT on 7 February to 12.00 GMT on the 8th. Although the aerosol-free layer appears to have fallen rather more rapidly than this its rate of descent is sufficiently uncertain to be in agreement with the synoptic trend.

5.2. 18–19 February 1983

The high-resolution profiles for this night are shown in Fig. 9. They show sharp ledges very similar to those of February 7/8, where the aerosol cloud effectively disappears in a 100 m height interval. With fewer profiles measured on this night and the obvious change in the profile of the cloud from 21.00 GMT to 06.00 GMT the upper edge of the main aerosol layer is less clearly identifiable as a tracer of atmospheric motions. Its fall of about 300 m in 9 hours was not consistent with the near-stationary position of the 475 K potential temperature surface over Camborne during the 24-hour period 12.00 GMT on the 8th to 12.00 GMT on the 9th. When compared with 7/8 February, this illustrates some of the danger inherent in the idea that sharp features in the aerosol cloud are inevitably tied to entropy surfaces, especially for periods in excess of 2–3 hours. From these two examples, it would therefore appear that the use of aerosol features as specific tracers should be restricted to periods of up to 1–2 hours.

6. Discussion and conclusions

This paper has investigated links between dynamical features in the atmosphere and measurements of the aerosol backscatter ratio at Aberystwyth during the early months of 1983. Because the El Chichon aerosol cloud had not distributed itself evenly around the globe at this time, frequent lidar observations provided a good opportunity to study its evolution with excellent height resolution. The onset and decay of a prominent tropospheric blocking episode during February 1983 were accompanied by very pronounced layering of the aerosol profiles, with changes by a factor of 7 in the backscatter ratio over 100 m. The change in the blocking pattern was manifest in the lower stratosphere as a transient planetary wave decaying in amplitude with height, giving favourable conditions for horizontal tracer gradients to be converted to vertical gradients by the mechanism of differential advection. The source of the aerosol-free layer near 19 km on February 7/8 could only be within the polar vortex (Fig. 8) and the creation at its boundaries of remarkably sharp vertical gradients in tracer concentration by differential advection must represent a mechanism for mixing air parcels from the two sides of the polar night jet maximum. Indeed, the evolution of the profiles over the observing night (Fig. 7) offers some evidence that mixing processes were eroding the layer, subject to the obvious caveat that observations at one site do not necessarily represent Lagrangian changes in the flow. Further sharp gradients were seen on 18/19 February (Fig. 9) when conditions were again favourable for differential advection. The gradients are much sharper than one would expect solely from a process such as an amplifying planetary wave, which in the stratosphere should always be very near to thermal wind balance and should not therefore cause abrupt vertical wind shears. Recent observations of winds near 29 km by Sidi and Barat (1986) have identified that inertial oscillations with short vertical wavelengths modify the overall wind profile, and a process such as this must be invoked to give a satisfactory explanation of our results. This combination of large-scale and small-scale differential advection appears to provide a mechanism for the destruction of cyclonic vortices (potential vorticity anomalies) displaced from the main winter polar vortex by planetary waves (McIntyre and Palmer, 1983; Clough et al., 1985).

Further evidence for the importance of large-scale differential advection is provided by comparing the Aberystwyth profiles during 2–4 February 1983 with the airborne lidar results of McCormick et al. (1983) over the Canadian Arctic. Above 20 km, the Aberystwyth profiles are consistent with airborne profiles within the polar vortex while below 20 km they are consistent with those outside. A sloping boundary to the vortex therefore seems likely.

7. Acknowledgements

We are indebted to Professor K. Labitzke of the Free University, Berlin, for supplying us with 30 mb and 50 mb charts, and to Dr. D. McKenna of the UK Meteorological Office for selected radiosonde data.

REFERENCES

Cadet, D. 1977. Energy dissipation within intermittent clear air turbulence patches. *J. Atmos. Sci. 34*, 137–142.

Clough, S. A., Graham, N. S. and O'Neill, A. 1985. Potential vorticity in the stratosphere derived using data from satellites. *Q. J. R. Meterorol. Soc. 111*, 335–358.

Heck, W. 1977. A comparison of estimated and directly measured turbulent heat fluxes in the lower stratosphere. *Mon. Wea. Rev. 105*, 1337-1340.

Hofmann, D. J. and Rosen, J. M. 1984. On the temporal variation of stratospheric aerosol size and mass during the first 18 months following the 1982 eruptions of El Chichon. *J. Geophys. Res. 89*, 4883–4890.

Hofmann, D. J., Rosen, J. M. and Gringel, W. 1985. Delayed production of sulfuric acid condensation nuclei in the polar stratosphere from El Chichon volcanic vapours. *J. Geophys. Res. 90*, 2341–2354.

Jeffreys, Sir Harold and Jeffreys, B. S. 1972. *Methods in mathematical physics*, 3rd edition, Cambridge University Press, U.K.

Kasten, F. 1968. Falling speed of aerosol particles, *J. Appl. Meteorol. 7*, 944–947.

Kent, G. S., Trepte, C. R., Farrukh, U. O. and McCormick, M. P. 1985. Variation in the stratospheric aerosol associated with the north cyclonic polar vortex as measured by the SAM II satellite sensor. *J. Atmos. Sci. 42*, 1536–1551.

Lejenäs, H. and Økland, H. 1983. Characteristics of Northern Hemisphere blocking as determined from a long time series of observational data. *Tellus 35A*, 349–361.

McCormick, M. P., Steele, H. M., Hamill, P., Chu, W. P. and Swissler, T. J. 1982. Polar Stratographic Cloud Sightings by SAM-II. *J. Atmos. Sci. 39*, 1387–1396.

McCormick, M. P., Trepte, C. R. and Kent, G. S. 1983. Spatial changes in the stratospheric aerosol associated with the north polar vortex. *Geophys. Res. Lett. 10*, 941–944.

McIntyre, M. E. and Palmer, T. N. 1983. Breaking planetary waves in the stratosphere. *Nature 305*, 593–600.

Naujokat, B., Petzoldt, K., Labitzke, K. and Lenschow, R. 1983. The first winter of Map — Dynamics, 1982/3, a winter with three different warming periods. Handbook for MAP volume 8, ed. C. F. Sechrist Jr.

Pinnick, R. G., Jennings, S. G. and Chyleck, P. 1980. Relationships between extinction, absorption, backscattering and mass content of sulfuric acid aerosols. *J. Geophys. Res. 85*, 4059–4066.

Reiter, E. R. 1972. Atmospheric transport processes. III, Hydrodynamic Tracers. AEC Critical Review Series, US Atomic Energy Commission.

Sidi, C. and Barat, J. 1986. Observational evidence of an inertial wind structure in the stratosphere. *J. Geophys. Res. 91*, 1209–1218.

Steele, H. M., Hamill, P., McCormick, M. P. and Swissler, T. J. 1983. The formation of polar stratospheric clouds. *J. Atmos. Sci. 40*, 2055–2067.

Thomas, L., Jenkins, D. B., Wareing, D. P. and Farrington, M. 1983. Laser radar observations in mid-Wales of aerosols from the El Chichon eruption. *Nature 304*, 248–250.

Thomas, L., Jenkins, D. B., Wareing, D. P., Vaughan, G. and Farrington, M. 1987. Laser radar observations of stratospheric aerosols associated with the El Chichon eruption. *Ann. Geophys. 5*, 47–56.

Wang, P. H. and McCormick, M. P. 1985. Variations in stratospheric aerosol optical depth during northern warmings. *J. Geophys. Res. 90*, 10597–10606.